American Mineralogist, Volume 71, pages 1434–1440, 1986

Crystal-chemical aspects of nonstoichiometric pyroxenes

Tamsin C. McCormick
Department of Geological Sciences, University of Colorado, Boulder, Colorado 80309-0250, U.S.A.

Abstract

Unit-cell parameters were determined for twelve mantle omphacites, at least eight of which are nonstoichiometric. The *a* and *b* cell dimensions and unit-cell volumes for the nonstoichiometric pyroxenes are consistently lower than would be expected for an ideal jadeite-diopside solution. Extrapolation to the Ca-Eskola endmember ($Ca_{0.5}\square_{0.5}AlSi_2O_6$) indicates a cell volume of 402 ± 5 Å^3 and a calculated density of 3.29 ± 0.04 g/cm^3 for this component. An X-ray structure refinement of an omphacite from the Bellsbank kimberlites, South Africa, revealed that vacancies are required in the structure in order for occupancies to be consistent with the mineral composition. Combined with electron-channeling results, the X-ray data indicate that the vacancies are largely constrained to the M2 site. The presence of vacancies does not appear to significantly affect the size of the M2 polyhedron under ambient temperature and pressure, although the M1 polyhedron of the vacancy-bearing pyroxene is substantially smaller than that predicted from endmember values.

Introduction

Analyses of omphacites commonly show marked deviations from the stoichiometric pyroxene formula. Those deviations reflecting a deficiency of cations appear greatest in highly aluminous pyroxenes from kyanite-bearing, mantle-derived eclogites and have been taken to indicate the presence of M-site vacancies (e.g., Wood and Henderson, 1978; Smyth, 1980). Pyroxenes that contain excess silica, and thus a cation : oxygen ratio of less than 2:3, have been synthesized under mantle conditions (e.g., Khanukhova et al., 1977; Wood and Henderson, 1978). Wood and Henderson (1978) have shown that the nonstoichiometry is stabilized by increasing pressure relative to stoichiometric pyroxene and quartz.

In the present study, an attempt was made to estimate the effect of nonstoichiometry on the density and crystal structure of pyroxenes. Refined unit-cell parameters were determined on a suite of omphacites from Roberts Victor and Bellsbank eclogites that cover a wide range of compositions. In order to characterize the vacancy distribution in a nonstoichiometric pyroxene, an X-ray structure refinement and channeling experiments were performed on an aluminous nonstoichiometric omphacite from a kyanite eclogite (SBB-1) from the Bellsbank kimberlites.

Unit-cell parameters and composition

The pyroxenes studied were analyzed by electron-microprobe wavelength-dispersive spectrometry, and in the case of SBB-1, several different combinations of standards were used in order to evaluate analytical errors. Garnets and pyroxenes within each sample were found to be chemically homogeneous. Microprobe analyses are given in Table 1, and data for SBB-1 are given in Table 2. The total Fe is reported as FeO, although clearly some of the Fe can be recalculated as Fe^{3+}, particularly in those analyses with cation totals of greater than four per six oxygens. It is also possible that some of the Fe may be trivalent in some of the vacancy-bearing pyroxenes, in which case the vacancy content could be higher than those values given in Tables 1 and 2.

Cell parameters were determined from single-crystal fragments by refining the setting angles for $K\alpha_1$ peaks for twelve to twenty reflections, between 32 and 67° 2θ (Mo radiation). Reflections were manually centered on a Picker four-circle diffractometer, and many of these were centered for both positive and negative 2θ. Cell parameters are presented in Table 1, and data for SBB-1 are given in Table 2.

The unit-cell parameters, plotted as a function of atomic Na/(Na + Ca), are shown in Figure 1. Also shown are X-ray data from Rossi et al. (1983) for a number of natural, stoichiometric *C*2/*c* omphacites. All of these pyroxenes contain only minor amounts of components other than diopside (Di), jadeite (Jd), and Ca-Eskola (CaEs). Kushiro (1969) suggested that mixing in the Jd-Di system is nonideal with molar volumes having slight positive deviation from ideal, although Wood et al. (1980) found pyroxenes on this join to show a linear variation of unit-cell volume with composition. Stoichiometric pyroxenes in this study and those of Rossi et al. (1983) presented in Figure 1 tend to have unit-cell volumes slightly larger than those predicted for an ideal mixture. In general, however, these pyroxenes have some Fe in addition to Di and Jd components, and this may account for their slightly larger unit cells. Unit-cell volumes from nonstoichiometric pyroxenes tend to plot below the straight line connecting

0003–004X/86/1112–1434$02.00

Table 1. Microprobe analyses and unit-cell parameters of mantle omphacites

	SBB-3P*	SBB-29	SBB-40	SBB-45	SBB-56	SBB-60	SBB-61	SBB-67	SRV-1**	SRV-6†	SRV-8†	SRV-12†	SRV-20†
No. of analyses	15	7	7	8	6	6	4	8	9	5	6	3	3
						Compositions in wt% (std. dev.) (n.d. = not determined)							
SiO_2	55.60(0.50)	55.93(0.29)	56.03(0.61)	55.43(0.91)	56.43(0.71)	55.18(1.12)	55.63(0.57)	54.65(0.90)	55.80(0.37)	57.30(0.19)	57.78(0.18)	56.23(0.21)	56.30(0.15)
TiO_2	0.05(0.05)	0.32(0.06)	0.35(0.05)	0.41(0.03)	0.34(0.04)	0.34(0.08)	0.28(0.02)	0.32(0.07)	0.09(0.05)	0.35(0.03)	0.44(0.02)	0.33(0.01)	0.37(0.02)
Al_2O_3	15.90(0.30)	14.03(0.24)	6.52(0.25)	7.92(0.14)	9.33(0.27)	9.23(0.30)	13.37(0.30)	4.07(0.26)	17.30(0.26)	17.24(0.09)	17.13(0.22)	14.09(0.21)	13.25(0.27)
Cr_2O_3	0.03(0.03)	0.31(0.04)	0.61(0.08)	n.d.	0.08(0.03)	0.14(0.04)	0.10(0.03)	0.84(0.07)	0.04(0.02)	0.03(0.03)	0.08(0.03)	0.11(0.04)	0.16(0.02)
FeO	1.02(0.05)	3.17(0.17)	5.55(0.09)	4.59(0.14)	4.22(0.36)	4.86(0.12)	2.38(0.15)	3.98(0.10)	1.68(0.07)	1.99(0.06)	1.60(0.07)	2.32(0.06)	2.56(0.08)
MnO	0.02(0.02)	0.03(0.02)	0.18(0.03)	0.09(0.06)	0.06(0.06)	0.05(0.03)	0.05(0.02)	0.11(0.03)	0.05(0.03)	n.d.	n.d.	0.04(0.01)	0.06(0.04)
MgO	7.10(0.14)	7.68(0.12)	12.65(0.25)	11.73(0.16)	10.62(0.10)	10.41(0.18)	8.50(0.18)	14.99(0.23)	5.99(0.22)	5.31(0.05)	6.39(0.18)	8.17(0.15)	8.43(0.16)
CaO	11.80(0.30)	11.36(0.27)	14.99(0.12)	14.16(0.12)	13.62(0.32)	14.79(0.27)	12.26(0.10)	17.58(0.43)	11.56(0.19)	10.97(0.26)	9.68(0.19)	11.75(0.11)	12.08(0.25)
Na_2O	7.85(0.18)	7.05(0.16)	4.56(0.10)	4.96(0.06)	4.96(0.10)	5.63(0.19)	6.22(0.25)	3.32(0.14)	6.80(0.23)	7.29(0.03)	8.29(0.11)	6.95(0.05)	6.56(0.05)
K_2O	0.00(0.00)	0.12(0.01)	0.15(0.02)	0.15(0.01)	0.15(0.03)	0.15(0.01)	0.13(0.01)	0.04(0.01)	0.22(0.03)	0.20(0.01)	0.22(0.02)	0.16(0.01)	0.16(0.01)
Total	99.37	100.00	101.59	99.44	99.81	100.78	98.92	99.90	99.53	100.68	101.61	100.15	99.93
						Cations per six oxygens							
Si	1.949	1.966	1.988	1.992	2.005	1.966	1.971	1.977	1.948	1.974	1.970	1.966	1.976
Ti	0.001	0.008	0.009	0.011	0.009	0.009	0.007	0.009	0.002	0.009	0.011	0.009	0.010
Al	0.657	0.581	0.273	0.335	0.391	0.388	0.558	0.174	0.712	0.700	0.688	0.581	0.548
Cr	0.001	0.009	0.017	—	0.002	0.004	0.003	0.024	0.001	0.001	0.002	0.003	0.004
Fe	0.030	0.093	0.165	0.138	0.125	0.145	0.071	0.120	0.049	0.057	0.046	0.068	0.075
Mn	0.001	0.001	0.005	0.003	0.002	0.002	0.002	0.003	0.001	—	—	0.001	0.002
Mg	0.371	0.402	0.669	0.628	0.562	0.553	0.449	0.808	0.312	0.273	0.325	0.426	0.441
Ca	0.443	0.428	0.570	0.545	0.518	0.565	0.465	0.682	0.432	0.405	0.354	0.440	0.454
Na	0.534	0.480	0.314	0.346	0.342	0.389	0.427	0.233	0.460	0.487	0.548	0.471	0.446
K	0.000	0.005	0.007	0.007	0.007	0.007	0.006	0.002	0.010	0.009	0.010	0.007	0.007
Total	3.987	3.974	4.018	4.005	3.964	4.027	3.958	4.032	3.928	3.914	3.953	3.972	3.965
Vacancy	0.013	0.026(9)	—	—	0.037(17)	—	0.042(12)	—	0.072(14)	0.086(4)	0.047(4)	0.028(3)	0.036(6)
						Unit-cell parameters‡							
a (Å)	9.549(5)	9.548(2)	9.656(3)	9.624(5)	9.619(5)	9.628(2)	9.561(3)	9.691(5)	9.553(9)	9.522(2)	9.520(4)	9.557(3)	9.562(7)
b (Å)	8.706(5)	8.721(1)	8.834(4)	8.795(4)	8.786(4)	8.806(2)	8.735(2)	8.863(3)	8.694(10)	8.696(1)	8.688(2)	8.732(2)	8.730(6)
c (Å)	5.249(6)	5.249(1)	5.253(2)	5.254(2)	5.248(2)	5.253(2)	5.252(2)	5.250(2)	5.231(5)	5.244(1)	5.245(3)	5.248(1)	5.249(2)
β (°)	106.86(6)	106.99(2)	106.61(3)	106.88(4)	106.87(3)	106.73(2)	107.00(3)	106.50(3)	107.17(8)	106.99(2)	107.09(4)	107.00(2)	106.97(4)
V (Å^3)	417.6(5)	418.0(1)	429.4(3)	425.5(3)	424.5(3)	426.6(2)	419.4(2)	432.4(3)	415.1	415.3(1)	414.6(3)	418.8(2)	419.2(4)
D (g/cm^3)	3.329	3.355	3.350	3.351	3.333	3.359	3.333	3.335	3.340	3.332	3.333	3.336	3.338

* Analysis from Smyth et al. (1984). ** Cell parameters from Smyth (1980). † Analyses from Smyth (1980). ‡ Errors in last figure in parentheses.

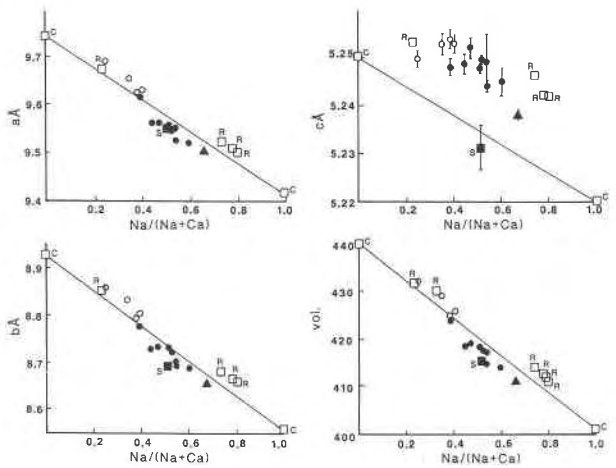

Fig. 1. Variation of unit-cell parameters with composition for nonstoichiometric (closed symbols) and stoichiometric (open symbols) pyroxenes. Error bars on c are ±1 estimated standard deviation. Squares labeled C, S, and R represent data of Cameron et al. (1973), Smyth (1980), and Rossi et al. (1983), respectively. The triangle represents the pyroxene used in the structure refinement.

cell parameters for diopside and jadeite. Although the unit-cell volume of Ca-Tschermaks pyroxene (CaTs) is significantly smaller than that of diopside (i.e., 421.35 Å^3; Okamura et al., 1974), the amounts of CaTs component in the pyroxenes in this study are insufficient to account for the smaller cell volumes. Mao (1971) also noted that extrapolation of unit-cell volumes of pyroxenes synthesized on the Jd-An (anorthite) join to the Ca-rich endmember gives a volume that is substantially lower than that of Ca-Tschermaks pyroxene.

An examination of a, b, and c as a function of composition shows that c is essentially constant over a range of compositions, whereas a and b display trends similar to those in the volume-composition plot. Again, stoichiometric pyroxenes all plot above the ideal Jd-Di join, whereas nonstoichiometric pyroxenes show slight negative deviation from an ideal trend.

The c cell parameter appears to be the least affected by the sizes of M1 and M2 cations. In their study in the CaO-MgO-Al_2O_3-SiO_2 (CMAS) system, Wood and Henderson (1978) found large decreases in c with increasing vacancies, but little effect on b. The presence of Al in tetrahedral sites appears to strongly affect c (e.g., Wood and Henderson, 1978). This may explain the large positive deviation in c for some of these pyroxenes, but does not account for the high c values of Rossi et al. (1983) for pyroxenes that have essentially no tetrahedral Al.

Calculated densities for each pyroxene are also presented in Table 1. Pure endmember diopside, jadeite, and Ca-Tschermaks pyroxene have densities of 3.28, 3.34, and 3.44 g/cm^3, respectively. Most of the pyroxenes in Table 1 have densities close to jadeite. Taking CaEs ($Ca_{0.5}\square_{0.5}AlSi_2O_6$) as the vacancy-bearing endmember and assuming ideal mixing, a cell volume of 402 ± 5 Å^3 is indicated for this component. This value is the same as that of Gasparik (1984) and falls in the range of estimates calculated from data of Wood and Henderson (1978). This would suggest a density of 3.29 ± 0.04 g/cm^3 for the hypothetical Ca-Eskola pyroxene at 1 bar and 25°C.

Table 2. Composition and cell parameters for SBB-1

	Average (of 18)	Std. dev.
SiO_2	57.09	0.39
TiO_2	0.36	0.05
Al_2O_3	19.83	0.25
Cr_2O_3	0.06	0.04
FeO	2.45	0.10
MnO	0.03	0.03
MgO	4.01	0.08
CaO	7.80	0.15
Na_2O	9.05	0.21
K_2O	0.07	0.02
Total	100.36	
Cations per six oxygens		
Si	1.957	0.008
Al^{IV}	0.043	0.008
Al^{VI}	0.758	0.006
Ti	0.009	0.001
Cr	0.002	0.001
Fe	0.070	0.003
Mn	0.001	0.001
Mg	0.205	0.004
Ca	0.286	0.004
Na	0.601	0.014
K	0.003	0.001
Vac	0.065	0.012

Note: Cell parameters (in ångströms; estimated errors in last figure are in parentheses): a = 9.501(1), b = 8.654(1), c = 5.238(1), β = 107.23(1)°, V = 411.4(1).

Crystal Structure

Compositional and structural considerations

The Bellsbank eclogite SBB-1, with pyroxene analyses showing a CaEs content of about 13%, was selected for the structural study. Microprobe analyses and cell parameters for the pyroxene are given in Table 2. The eclogite is fresh, with slight alteration evident only along grain boundaries.

The suggestion that this pyroxene contains vacancies is based on some assumptions. The most important of these is that the microprobe analyses reflect the true composition of the pyroxene. Standard deviations in Table 2 should account for all analytical errors and for chemical inhomogeneity. Energy-dispersive spectrometry revealed no other elements in significant abundance. The presence of a light element such as Li or Be would, however, go undetected in the microprobe. Hervig (1984, pers. comm.) analyzed SBB-1 pyroxene for light elements using the ion microprobe and found less than 100 ppm Li_2O, 5 ppm BeO, and 10 ppm B_2O_3. These quantities are insufficient to account for the cation deficiency in this sample.

An additional assumption is that the pyroxene is a single-chain silicate, with none of the double or triple chains described by Veblen and Buseck (1981). An apparent cat-

Table 3. Atomic coordinates and anisotropic thermal parameters for SBB-1

	M1	M2	Si	O1	O2	O3
x/a	0.00000	0.00000	0.28947(4)	0.11043(9)	0.3608(1)	0.35291(9)
y/b	0.90540(5)	0.30090(6)	0.09297(3)	0.0779(1)	0.2601(1)	0.0108(1)
z/c	0.25000	0.25000	0.22831(6)	0.1309(2)	0.3005(2)	0.0034(2)
β_{11}	0.00120(5)	0.00313(7)	0.00094(3)	0.00106(9)	0.00279(9)	0.00146(8)
β_{22}	0.00161(6)	0.00204(7)	0.00137(4)	0.0029(1)	0.00183(9)	0.0028(1)
β_{33}	0.0039(2)	0.0056(2)	0.0030(1)	0.0078(3)	0.0080(3)	0.0048(3)
β_{12}	0.00000	0.00000	−0.00006(3)	0.00016(7)	−0.00045(8)	0.00012(7)
β_{13}	0.00053(7)	−0.00031(9)	0.00065(5)	0.0009(1)	0.0012(1)	0.0010(1)
β_{23}	0.00000	0.00000	−0.00017(4)	−0.0005(1)	−0.0006(1)	−0.0011(1)

ion deficiency of 0.025 per six oxygens would result from 10% amphibole lamellae in the pyroxene (Veblen and Buseck, 1981). In order to check for the presence of multiple chains, a fragment of the pyroxene was examined by high-resolution transmission electron microscopy using a Philips 400T microscope. No multiple chains were observed in the images. In addition, the sharp X-ray diffraction peaks produced by the crystal used in the structure refinement are inconsistent with a high abundance of multiple chains.

Experimental method

A fragment of a centimeter-sized grain was selected for X-ray study, and a larger fragment of the same grain was oriented and ion-thinned for observation by transmission electron microscopy. Long-exposure precession photographs confirmed the space group as $C2/c$. Omphacites with lower symmetry are common in metamorphic eclogites, and they may show complex ordering and exsolution transformations (e.g., Carpenter, 1980). However, no low-symmetry omphacites are known from kimberlite inclusions.

The crystal fragment used in the structure refinement approximates a triangular prism about 100 μm thick and 250–280 μm long on each side of the triangular face. Intensity data for hkl, $h + k$ even, were collected on a Syntex four-circle diffractometer. A total of 3241 reflections were measured, including all eight quadrants up to 60° 2θ and four quadrants from 60 to 70° 2θ. Intensities from two standard reflections, collected every 100 reflections, had standard deviations within counting statistics.

In order to check absorption corrections, ψ-scans were performed on six reflections between 24 and 48° 2θ, with maximum deviations about χ of ±18°. Variance of up to 35% of the observed intensities was evident in the ψ-rotations. Numerical corrections for absorption were made on the basis of the crystal shape. The relative standard deviations of ψ-scan intensities were reduced to within counting statistics for most of the reflections after applying absorption corrections. However, due to the complex shape of the crystal, slight residual systematic error is evident.

After correcting for Lorentz and polarization factors and for absorption, the intensity data were averaged, producing 914 independent reflections with an R factor for averaging of F^2 of 2.3%. Examination of those reflections showing largest standard deviations for averaging did not reveal any obvious trend as a function of 2θ or hkl. Thus, no systematic sources for residual inconsistencies could be determined.

Refinements

Initial crystal-structure refinements were done using Sheldrick's SHELX program package, modified for implementation at the University of Colorado, Boulder. Reflections for which $F^2 \leq 3\sigma(F^2)$ were suppressed, resulting in 830 independent, observed reflections. Subsequent refinements were done in which no reflections were suppressed, using RFINE (Finger and Prince, 1975). Scattering factors were taken from the *International Tables for X-ray Crystallography,* Volume IV, using values for O^{1-}, Fe^{2+}, and fully ionized species for other elements.

The main questions to be addressed with the refinements were whether the structure is likely to contain vacancies and what the vacancy distribution might be. To answer the first question, a vacancy model was compared with an alternative model in which all sites are fully occupied. The second question was addressed by refining two different models for the vacancy distribution.

The final refinement of the second vacancy model was done assuming $Si^{1.5+}$ and $O^{1.5-}$ as the Si and O scattering species, using the scattering factor for O^{2-} from Tokonami (1965). Results of this final refinement of anisotropic temperature factors, scale, atomic positions, and Mg and Fe distribution for the second vacancy model are shown in Table 3. Observed and calculated structure factors for this last cycle are presented in Table 4.[1] Occupancies for M1 and M2 from each of the refinements are shown in Table 5.

For the model with no vacancies, Fe and Al^{VI} were constrained to M1, and Ca and Na were constrained to M2, although their proportions were allowed to vary. Mg_{M1} was included with Al and Mg_{M2} was included with Na, to simplify the refinement. The differences in scattering factors between these species are considered to be small enough not to significantly affect the conclusions. The results of refining the occupancies of Ca, Fe, Mg + Al and Mg + Na, such that M1 and M2 total occupancies are both 100%, are shown in Table 5. Although anisotropic temperature factors were also allowed to vary, they did not change significantly from the vacancy model.

Vacancy models were refined using atomic proportions from the microprobe analyses. Na and Ca were placed in M2 and Al in M1. Owing to the problem of simultaneously refining M1 and M2 occupancies of three species (Mg, Fe,

[1] To receive a copy of Table 4, order Document AM-86-318 from the Business Office, Mineralogical Society of America, 1625 I Street, N.W., Suite 414, Washington D.C. 20006, U.S.A. Please remit $5.00 in advance for the microfiche.

Table 5. Occupancies for M sites in SBB-1 omphacite

	Full-occupancy model		Vacancy model I*		Vacancy model II**	
Atom	M1 occ.	M2 occ.	M1 occ.	M2 occ.	M1 occ.	M2 occ.
Fe	0.069(4)	0.000	0.082	0.000	0.063(2)	0.019(2)
Ca	0.000	0.229(7)	0.000	0.286	0.000	0.286
Al	0.931(4)	0.000	0.758	0.000	0.758	0.000
Mg	—†	—†	0.136(3)	0.069	0.179(2)	0.026(2)
Na	0.000	0.770(7)	0.000	0.602	0.000	0.602
Total	1.000	0.999	0.976	0.957	1.000	0.933
	$R = 0.027$	$R_{wt} = 0.052$	$R = 0.026$	$R_{wt} = 0.036$	$R = 0.023$	$R_{wt} = 0.028$

* All Fe in M1.
** All vacancies in M2.
† Mg_{M1} included with Al; Mg_{M2} included with Na.

and vacancies), models to be tested required fixing some of these parameters. In the first refinement, Fe was constrained to be in M1, and Mg and vacancy populations allowed to vary between M1 and M2. The resulting occupancies (shown in Table 5) indicated twice as many vacancies in M2 as there are in M1. The presence of vacancies in M1 indicates an attempt to reduce the overall scattering for M1. Therefore, a second model was tested, in which all the vacancies were placed in M2, and Fe and Mg were allowed to vary between M1 and M2.

Comparing the results of the refinements in Table 5, it is apparent that in the full-occupancy model the total scattering factor for each site was maintained by increasing the proportions of elements with lower Z. The sum of the light elements (Al^{VI}, Mg, and Na) in the full-occupancy model is significantly higher (at the 99% confidence level) than in the vacancy model, and the heavier elements are significantly lower. The chemistry for the nonvacancy model is inconsistent with the electron-microprobe analyses, and thus the preferred model is that in which the M sites are not fully occupied.

Comparing the two vacancy models, it can be seen that in the model with all the vacancies in M2, about 22% of the Fe moved from M1 to M2 in order to lower the total scattering for M1. Both models initially refined to $R = 0.026$ and $R_{wt} = 0.036$. They also both showed substantial contribution to the R coming from the low-angle reflections, but the R value for successive shells of reciprocal space was the same in each model. The low-angle reflections usually include the most intense reflections, which may also be subject to extinction problems. The low sin θ/λ part of the total scattering curve depends more on the total number of electrons for a site and not on the nature of the scattering species. Rossi et al. (1983) noted that large discrepancies in reflections with sin $\theta/\lambda < 0.3$ could be eliminated by using scattering factors for $Si^{1.5+}$ and $O^{1.5-}$, although these scattering factors gave the same atomic positions, occupancies, and thermal parameters as those obtained using only data with sin $\theta/\lambda > 0.3$. Refinements of the second vacancy model for this crystal using these scattering factors reduced the R for the 46 lowest-angle reflections from 0.066 to 0.043. The final R for all reflections was 0.023, and R_{wt} was 0.026. Atom positions and occupancies did not change, but temperature factors were reduced for M1, M2, and all three oxygens. Thermal ellipsoids showed the same orientations as those from the earlier refinements, although the amplitudes were substantially reduced.

Electron channeling

A technique for quantitative determination of site occupancies in minerals, based on channeling-enhanced emission of characteristic X-rays, has recently been applied to a number of minerals including pyroxenes (Self et al., 1983). Calculations show that fairly strong differences in X-ray emission from M1 + T and M2 sites in clinopyroxenes can be achieved by tilting crystals slightly about the Bragg angle for the (020) reflection (Self et al., 1983; M. T. Otten, 1985, pers. comm.).

A fragment of the vacancy-bearing pyroxene from the SBB-1 eclogite was oriented using a precession camera, and an ion-thinned sample prepared for TEM work. A Philips 400 TEM, operating at 120 kV and fitted with a Kevex energy-dispersive X-ray spectrometer, was used for the experiments. The crystal was oriented so that only the (0k0) systematic row showed strong intensity. Spectra were collected from the crystal when it was oriented so that the electron beam was inside the Bragg angle for (020) (symmetric position), and subsequently when the beam was slightly outside the Bragg angle for (020) (i.e., the crystal tilted to slightly beyond the two-beam condition). In these two orientations, X-ray emission is enhanced from the M1 + T sites and the M2 sites, respectively.

Measured peak intensities were ratioed to Si for each spectrum and values of $R = (X/Si)_{>\theta}/(X/Si)_{<\theta}$ determined for each element. Owing to problems of peak deconvolution and background subtraction for the low-energy part of the spectrum and possible Na migration during analysis, no attempts were made at quantitative analysis. However, repeat analyses show consistently $R_{Na} \simeq R_{Ca} > R_{Fe} > R_{Mg} \geq R_{Al}$. The values of R for Al are close to 1.0 indicating that all the Al is on the M1 and T sites. The site preference for M2 for each element is indicated by its relative R value. The channeling experiments suggest that the proportion of Fe in M2 is greater than the proportion of Mg in M2. These two values from the structure refine-

Table 6. Ellipsoids of vibration for SBB-1 omphacite

Atom	Axis	RMS amplitude	Angle (°) with **a**	Angle (°) with **b**	Angle (°) with **c**	Equivalent isotropic *b*
M1	1	0.069	54	90	53	0.479
	2	0.073	36	90	143	
	3	0.078	90	0	90	
M2	1	0.078	72	90	34	0.796
	2	0.088	90	180	90	
	3	0.128	163	90	55	
Si	1	0.581	138	87	31	0.335
	2	0.063	129	112	118	
	3	0.074	103	22	103	
O1	1	0.065	11	97	99	0.669
	2	0.096	87	123	144	
	3	0.109	100	146	56	
O2	1	0.078	74	24	78	0.764
	2	0.103	79	75	164	
	3	0.112	19	108	100	
O3	1	0.067	126	67	32	0.598
	2	0.079	142	95	110	
	3	0.110	100	156	66	

Table 7. Bond distances and polyhedral volumes for SBB-1 omphacite

	SBB-1	Predicted*
Si–O1	1.630	1.623
Si–O2	1.595	1.590
Si–O3	1.637	1.643
Si–O3	1.653	1.658
M1–O1	2.026	2.043
M1–O1	1.966	1.990
M1–O2	1.899	1.931
M1 V (Å^3)	9.918	10.362
M2–O1	2.368	2.358
M2–O2	2.394	2.388
M2–O3	2.419	2.444
M2–O3	2.734	2.731
M2 V (Å^3)	24.968	25.052

* $Jd_{60}Di_{40}$ based on endmember values in Cameron et al. (1973).

ment with all vacancies in M2 are 22% for Fe and 13% for Mg. Therefore the channeling experiments are consistent with the vacancy model in which all the vacancies are in M2. In fact, if one develops a model in which the proportions of Fe and Mg are equal on both sites, assuming the Fe is Fe^{2+}, still less than 10% of the vacancies would reside in M1. Thus on the basis of the channeling results, one may conclude that more than 90% of the vacancies are in M2.

Discussion

Parameters for thermal ellipsoids of each atom from the X-ray structure refinement are given in Table 6. Bond distances are presented in Table 7, together with those predicted for pyroxene with composition $Jd_{60}Di_{40}$, based on a linear interpolation between endmember values from Cameron et al. (1973). Rossi et al. (1983) have noted some problems in predicting crystal-chemical properties of intermediate compositions, based on endmember values. However, measured M–O bond distances and M1 polyhedral volumes for their $C2/c$ pyroxenes are in close agreement with such interpolations. The M1–O bond distances are all smaller for the pyroxene in this study, and consequently, M2–O1 and M2–O2 bond distances are slightly longer than those predicted for an ideal $Jd_{60}Di_{40}$ pyroxene. The calculated polyhedral volume for M1 octahedra for SBB-1 is about 4% smaller than the predicted value, although the higher Al^{VI} content due to the CaTs and CaEs components does not alone account for this discrepancy. The volume for M2 polyhedra is similar to the predicted value. The similarity between the observed and predicted parameters for M2 would suggest that partial occupancy of M2 does not significantly affect the size of this coordination polyhedron at ambient temperature and pressure, although there may be an effect on the volume of M1.

In an X-ray study of nonstoichiometric pyroxenes from the Zagadochnaya kimberlite, Smith et al. (1982) reported that their results are consistent with, but do not prove, the existence of vacancies in M2. However, it is believed that the comparison of the full-occupancy model with the vacancy model leaves little doubt that vacancies are present in the structure. The results of the final refinements and the channeling experiments indicate that the vacancies are in M2.

It is possible that some of the Fe may be trivalent. If one considers all the Fe in the crystal to be trivalent, there would be over 8% vacancies in the structure, based on stoichiometry. It is likely that Fe^{3+} would reside in M1. Consequently, the structure would approximate vacancy model I in Table 5, except that the low-angle scattering of Fe^{3+} is slightly less than that of Fe^{2+} and thus Mg would move to M1 from M2. Calculations suggest that not more than about 18% of the vacancies could occur in M1 in such a model.

The vacancy endmember is generally taken as CaEs, and this is supported by the findings of this study. It is not known how the distribution of vacancies varies with composition, but it is possible that the partitioning of vacancies between M1 and M2 may depend on other cations present in the M sites. If this is the case, two vacancy endmembers may be needed to fully describe a pyroxene. However, further structure refinements would be required to determine the M-site occupancies.

Conclusions

Unit-cell volumes of nonstoichiometric pyroxenes are consistently lower than would be expected for an ideal solution between jadeite and diopside. An estimate of the cell volume of the hypothetical vacancy-bearing endmember, Ca-Eskola pyroxene ($Ca_{0.5}\square_{0.5}AlSi_2O_6$), is 402 ± 5 Å^3, corresponding to a density of 3.29 ± 0.04 g/cm^3 at 1 bar and 25°C. The parameters for Ca-Eskola pyroxene under mantle conditions are unknown, but it is possible that vacancy-bearing pyroxenes may have distinctly different compressibilities than stoichiometric pyroxenes. The smaller cell volume of nonstoichiometric pyroxenes also

suggests that CaEs is stabilized by high pressure relative to stoichiometric pyroxene and quartz or anorthite and quartz. Therefore, it is possible that vacancy-bearing pyroxenes are abundant in the lower parts of the upper mantle.

A crystal-structure refinement of a nonstoichiometric omphacite indicates that the structure is likely to contain vacancies. Electron channeling experiments indicate that the proportion of Fe in M2 is greater than the proportion of Mg in M2. Combining these results with those of the crystal-structure refinements, it appears that all the vacancies reside in M2. Therefore CaEs would appear to be an appropriate endmember to describe vacancy-bearing pyroxenes.

Acknowledgments

The current investigation was started as part of a Ph.D. degree at Arizona State University and has taken place in a number of different places over a number of years. Microprobe analyses, unit-cell determinations, and electron-channeling experiments were done at Los Alamos National Laboratory (the latter at the Center for Materials Science). Curt Haltiwanger (University of Colorado, Boulder) is gratefully acknowledged for collecting the X-ray intensity data and for help with initial structure refinements. Rick Hervig (Arizona State University) analyzed samples on the ion microprobe (established under NSF Grant DMR8206028 to Peter Williams). High-resolution electron microscopy was done at the ASU Facility for High Resolution Electron Microscopy. Joe Smyth is gratefully acknowledged for providing samples, allowing access to unpublished data, and for invaluable discussions throughout. Reviews by T. Gasparik and B. Wood are acknowledged. Financial support was provided through Grants EAR8408168 (to Peter Buseck, ASU) and EAR8318674 (to Joseph Smyth, University of Colorado).

References

Cameron, M., Sueno, S., Prewitt, C.T., and Papike, J.J. (1973) High-temperature crystal chemistry of acmite, diopside, hedenbergite, jadeite, spodumene and ureyite. American Mineralogist, 58, 594–618.

Carpenter, M.A. (1980) Mechanisms of exsolution in sodic pyroxenes. Contributions to Mineralogy and Petrology, 71, 289–300.

Finger, L.W., and Prince, E. (1975) A system of Fortran IV computer programs for crystal structure computations. National Bureau of Standards Technical Note 854.

Gasparik, Tibor. (1984) Experimental study of subsolidus phase relations and mixing properties of pyroxene in the system CaO-Al_2O_3-SiO_2. Geochimica et Cosmochimica Acta, 48, 2537–2545.

Khanukhova, L.T., Zharikov, V.A., Ishbulatov, R.A., and Litvin, Yu.A. (1977) The surface of saturation of clinopyroxenes with silica in the system $CaMgSi_2O_6$-$NaAlSi_2O_6$-$CaAl_2SiO_6$-SiO_2 at 35 kilobars and 1200°C. Doklady Akademii Nauk SSSR, 234, 175–179.

Kushiro, Ikuo. (1969) Clinopyroxene solid solutions formed by reactions between diopside and plagioclase at high pressures. Mineralogical Society of America Special Paper 2, 179–191.

Mao, H.K. (1971) The system jadeite ($NaAlSi_2O_6$)–anorthite ($CaAl_2Si_2O_8$) at high pressures. Carnegie Institution of Washington Year Book 69, 163–168.

Okamura, F.P., Ghose, S., and Ohashi, H. (1974) Structure and crystal chemistry of calcium Tschermak's pyroxene $CaAlAlSiO_6$. American Mineralogist, 59, 549–557.

Rossi, G., Smith, D.C., Ungaretti, L., and Domeneghetti, M.C. (1983) Crystal-chemistry and cation ordering in the system diopside-jadeite: A detailed study by crystal structure refinement. Contributions to Mineralogy and Petrology, 83, 247–258.

Self, P.G., Spinnler, G.E., and Buseck, P.R. (1983) Pyroxenes—A novel case for atomic site occupancy determination by Alchemi. Geological Society of America Abstracts with Programs, 15, 683.

Smith, D.C., Domeneghetti, M.C., Rossi, G., and Ungaretti, L. (1982) Single-crystal structure refinements of super-silicic clinopyroxenes from the Zagadochnaya kimberlite pipe, Yakutia, USSR. Terra Cognita, 2, 223.

Smyth, J.R. (1980) Cation vacancies and the crystal chemistry of breakdown reactions in kimberlitic omphacites. American Mineralogist, 65, 1185–1191.

Tokonami, Masayasu. (1965) Atomic scattering factor for O^{2-}. Acta Crystallographica, 19, 486.

Veblen, D.R., and Buseck, P.R. (1981) Hydrous pyriboles and sheet silicates in pyroxenes and uralites: Intergrowth microstructures and reaction mechanisms. American Mineralogist, 66, 1107–1134.

Wood, B.J., and Henderson, C.M.B. (1978) Composition and unit cell parameters of synthetic non-stoichiometric tschermakitic clinopyroxenes. American Mineralogist, 63, 66–72.

Wood, B.J., Holland, T.J.B., Newton, R.C., and Kleppa, O.J. (1980) Thermochemistry of jadeite-diopside pyroxenes. Geochimica et Cosmochimica Acta, 44, 1363–1371.

Manuscript received January 2, 1986
Manuscript accepted July 8, 1986